ChemComm

Chemical Communications

Accepted Manuscript

This article can be cited before page numbers have been issued, to do this please use: K. Salome and C. F. Tormena, *Chem. Commun.*, 2019, DOI: 10.1039/C9CC04268G.

ROYAL SOCIETY OF CHEMISTRY

rsc.li/chemcomm

View Article Online
DOI: 10.1039/C9CC04268G

COMMUNICATION

Enantiodiscrimination by Matrix-Assisted DOSY NMR

Kahlil Schwanka Salome[a] and Cláudio Francisco Tormena*[a]

Received 00th January 20xx,
Accepted 00th January 20xx

DOI: 10.1039/x0xx00000x

High-resolution NMR is an essential technique for structure determination, however, stereochemistry assignment is still an obstacle. Several methods are known to overcome this limitation but usually at high costs or using derivatizations. Here we described the use of different solvating agents to virtually discriminate the enantiomers of 15 analytes using ^{1}H and ^{19}F-{^{1}H} DOSY NMR.

Nuclear Magnetic Resonance (NMR) is arguably one of the best techniques for structural elucidation of pure compounds in isotropic solutions, once it is possible to obtain information about atoms connectivity and relative stereochemistry.[1] However, to attain enantiodiscrimination, it is necessary to change one of the enantiomers chemical environment by adding an enantiopure compound such as chiral derivatizing agents (CDAs), chiral lanthanide shift reagents (CLSRs),[2] chiral liquid crystals[3] or chiral solvating agents (CSAs)[4] to create a diastereotopic environment. CSAs have great advantages due to non-covalent interaction with the compound under investigation, enabling the recovery of it at the end of the analysis. The CSAs are easier to use and the signals are not broadened due to the presence of any paramagnetic nucleus.[5] There are several reports of CSAs such as hydrogen bonding agents,[6] metal complexes,[7] macrocyclic reagents,[8] and many others,[9] but most of the CSAs are not commercially available, and in the case where are available they are expensive, only water-soluble or are applied for a specific class of enantiomers such as carboxylic acids and amines. Even though chiral alcohols are widely synthesized, there are a few cases of enantiodiscrimination of alcohols using CSAs and even fewer of analysis at room temperature.[10] Nevertheless, even for an ideal CSA, there is a downside of adding another compound to the enantiomeric mixture. The introduction of new signals in the NMR spectrum might cause signal overlapping, mainly in the ^{1}H spectrum. To overcome this, NMR methods have been developed to complex mixture analysis and one of the most popular among many fields of study is the Diffusion-Ordered SpectroscopY (DOSY),[11] this technique has the potential of eliminating laborious purification procedures and allows the identification of compounds directly in mixtures.[12,13] However, dealing with compounds of same molecular weight and hydrodynamic radii is a serious limitation in DOSY measurements. In this case, a compound (like a CSA) can be used to separate the signals in the acquisition dimension and thus improve the separation of compounds in the diffusion dimension. This technique is called Matrix-Assisted DOSY (MAD)[14] and is employed to differentiate compounds with the same diffusion coefficient, such as isomers, and analyse the efficiency and versatility of chiral auxiliaries without the need of previous purification.[15] Here we describe the use of 5 CSAs (of three different types) in the chiral discrimination of 17 different compounds using MAD (Fig. 1). CSAs **1-2** (binaphthyl with hydroxyl groups) and **3-4** (binaphthyl with diphenylphosphine groups) are very simple, widely used in asymmetric synthesis[16] and commercially available for an accessible price. The CSA **5** (large binaphthyl derivative) is also available and, even though it is more expensive, it was chosen to measure the influence of a larger CSA in the separation of compounds in the diffusion dimension. The analytes were chosen to cover a range of different possible interaction between analytes and CSAs.

In order to measure the chiral solvating capacity of BINOL, six samples were prepared using 21.9 mmol L^{-1} of camphor **(8/9)** and 0, 1, 2, 3, 4 and 5 equivalents of **2** in $CDCl_3$, in which the CSA starts to be insoluble. The best separation of signals was achieved when 5 equivalents of the CSA was used (Fig. 2), and this ratio was used for all the analysis with CSAs **1-4**. For **5** the ratio was kept in 1:1 due to availability of compound. Then, in an attempt to improve the signals separation, the 1D NMR experiments were carried out in various temperatures and solvents with different polarities. It was observed that a reduction in temperature shifted the equilibrium towards the formation of a complex between analytes and CSA agent

[a] *Institute of Chemistry, University of Campinas - UNICAMP, P.O. Box 6154, 13083-970 Campinas, SP, Brazil.* tormena@unicamp.br

† Footnotes relating to the title and/or authors should appear here.

Electronic Supplementary Information (ESI) available: [details of any supplementary information available should be included here]. See DOI: 10.1039/x0xx00000x

leading to improvement in separation in the ^{1}H dimension (Fig. 3).

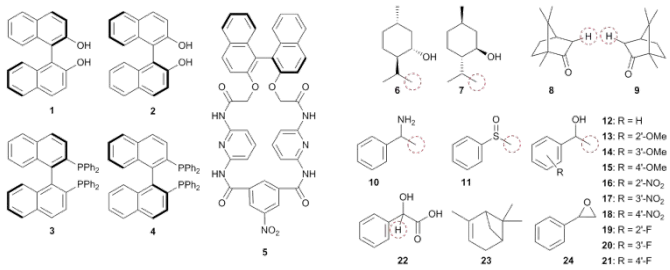

Fig. 1: chemical structure of matrices (**1**-**5**) and analytes (**6**-**24**). The red circles represent the selected hydrogens monitored by DOSY.

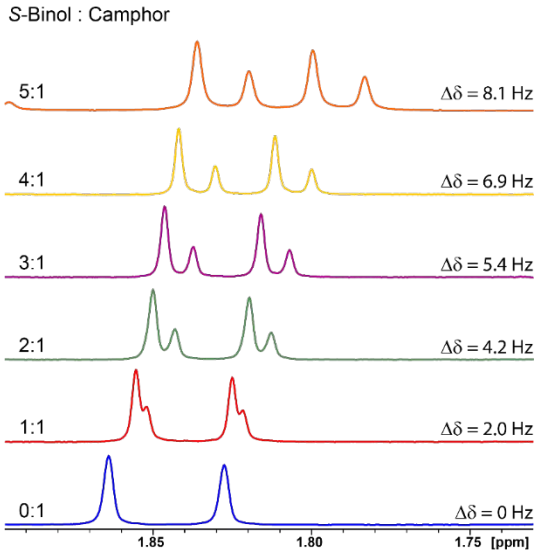

Fig. 2: Δδ values of diastereoisomeric complexes of (*S*)-BINOL and camphor in different ratio (from 0:1 to 5:1) with an excess of (*S*)-camphor enantiomer.

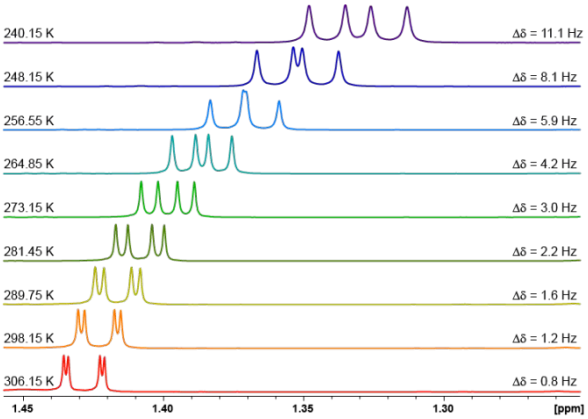

Fig. 3: Δδ values of ^{1}H NMR signal of the methyl group of 4'-fluoro-1-phenylethanol (racemic) in a diastereoisomeric complex with (*S*)-BINOL at different temperatures.

In limit cases, reducing temperature must be used to improve the differentiation, but to avoid convection effects[17] on DOSY measurements the remaining experiments were performed at 25 °C. The effect of solvent polarity in the differentiation between enantiomers was investigated, and separation of the diastereoisomer species on ^{1}H and ^{19}F-{^{1}H} spectra suggests that increasing the polarity decreases the efficiency of separation (Fig. 4). This effect is due to the competing interactions between CSAs and analytes and CSAs and a polar solvent. With all parameters involved in differentiation efficiency optimized, ^{1}H and ^{19}F-{^{1}H} were acquired in $CDCl_3$, at 25 °C, and the measured Δδ between the diastereoisomeric pair are summarized in Table 1 (the experimental NMR parameters are described in ESI).

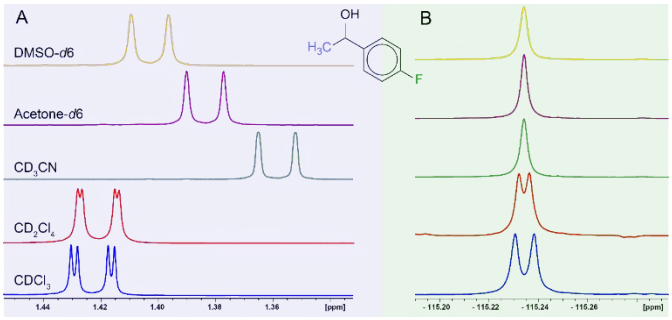

Fig. 4: 4'-fluoro-1-phenylethanol (racemic) and (*S*)-BINOL in different solvents. A) ^{1}H NMR spectra and B) ^{19}F-{^{1}H} spectra.

Table 1: Δδ (Hz) values between the diastereoisomeric pair of selected protons of compounds **6-21** with matrices **1-5** in $CDCl_3$, at 25 ºC.

Entry	Compound	CSA				
		1	2	3	4	5
1	**6/7**	1.1	1.1	0.0	0.0	-
2	**8/9**	8.1	8.1	0.0	0.0	3.8
3	**10**	22.7	22.5	0.0	0.0	-
4	**11**	10.1	9.0	0.0	0.0	-
5	**12**	0.8	0.8	0.0	0.0	-
6	**13**	1.3	1.1	0.0	0.0	-
7	**14**	1.5	1.2	0.0	0.0	-
8	**15**	0.7	0.7	0.0	0.0	-
9	**16**	4.8	4.6	0.0	0.0	-
10	**17**	0.0	0.0	2.2	2.0	-
11	**18**	1.2	1.3	1.9	2.0	-
12	**19** (^{1}H)	0.7[a]	0.8[a]	0.4	0.4	3.9
13	**19** (^{19}F-{^{1}H})	0.0	0.0	0.0	0.0	67.8
14	**20** (^{1}H)	0.7	0.6	0.0	0.0	2.0
15	**20** (^{19}F-{^{1}H})	2.2	2.1	0.0	0.0	10.3
16	**21** (^{1}H)	1.7	1.8	0.0	0.0	0.0
17	**21** (^{19}F-{^{1}H})	5.2	5.6	0.0	0.0	54.6
18	**22**	4.7	4.7	2.5	2.6	96.4
19	**23**	0	0	0	0	-
20	**24**	0	0	0	0	-

[a] Δδ obtained using a ^{1}H-{^{19}F} pulse sequence

The menthol (**6/7**), samples containing 20% of enantiomeric excess of each enantiomer were mixed with (*R*) or (*S*)-BINOL resulting in four samples: (*R*) or (*S*)-BINOL with (+)-menthol excess and (*R*) or (*S*)-BINOL with (-)-menthol excess. Comparing the ^{1}H spectra of these samples (Fig. S1) we can observe that (*S*)-BINOL has a greater shielding effect for methyl group of (-)-menthol in comparison to (+)-menthol, while (*R*)-BINOL shields the methyl group of (+)-menthol better than (-)-menthol. This result is very similar to camphor (**8/9**): (*R*)-BINOL shields (*R*)-camphor better than (*S*)-camphor and the shielding effect of (*S*)-BINOL is greater on (*S*)-camphor. This effect was observed for

all analytes except for 3'-nitro-1-phenylethanol (**17**), which showed no separation of signals using BINOL (Table 1, entry 10).

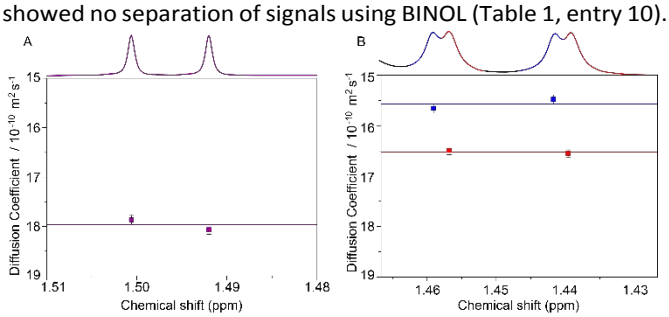

Fig 5. 500 MHz ^{1}H DOSY, with the least attenuated 1D spectrum shown at the top, for: **a)** compound **12; b)** compound **12** containting CSA **2** showing the difference in diffusion coefficients with and without the CSA

On the other hand, using BINAP the separation of diastereoisomeric complexes signals was observed only in a few compounds: **18**, **19** and **22** (Table 1, entries 10, 11 and 18). The $\Delta\delta$ values are related to the efficiency of diastereoisomeric separation but these $\Delta\delta$ values give no information on which enantiomer forms a stronger diastereoisomeric complex with the CSA, since the chemical shift depends only on the chemical environment of the observed proton. In a complex, the chemical shift of the observed protons will depend on the stability (lifetime) of formed complex between analytes and CSA, more specifically, on the proximity of the atom of interest and the shielding effect of the naphthyl groups in the case of Binol as CSA agent.

Therefore, to get more information on which enantiomer will bind more strongly with the CSA, or in other words, the enantioselectivity of the CSA, the DOSY spectra must be analysed. Fig. 5 illustrates the difference in diffusion coefficients when the CSA is added to the sample. Both enantiomers have the same D in the absence of CSA (Fig. 5a) and, when CSA is added, both D are reduced, as each diastereoisomer complex is larger than either SA or enantiomer separately.

However, the interaction of each enantiomer occurs in different extension (strength), which results in different diffusion coefficients for each diastereoisomeric pair, enabling the discrimination of the enantiomers. The differences in diffusion values (ΔD) of different diastereoisomeric complexes were calculated following the example on Fig. 5 and are reported in Table S1, diffusion maps along with diffusion coefficients and an example of ΔD calculation are also available in the Support Information (Fig S2-S44).

The difference in diffusion coefficients is quite small (Table S1) and, in some cases, very close to the error bar, when BINOL or BINAP were used. Even though the ΔD are small, this result is expected at first glance once there is a great overlap of signals in most cases. However, when using CSA **5**, which is substantially larger than the others, the $\Delta\delta$ values are larger than using CSAs **1-4** (Table 1), but this separation isn't necessarily reflected in better separation in the diffusion dimension.

In systems presenting large $\Delta\delta$, the D values can be properly measured and thus, ΔD values are exact. However, if the $\Delta\delta$ is small (the signals are overlapping) the fitting of the exponential decay of each signal will be contaminated by the decay of the other signal. In theory, comparing the same sample, the ΔD is zero for a completely overlapped pair of signals and it grows with the $\Delta\delta$ until it reaches a maximum value for entirely separated signals. This means D values measured with overlapping signals are not exact and the calculated ΔD is underestimated. And comparing different samples, there is no correlation between $\Delta\delta$ and ΔD.For the aliphatic compounds (**6-9**), the diffusion results are analogous, even with only 1.1 Hz of separation in the ^{1}H NMR spectrum for **6** and **7** and 8.1 Hz of separation for **8** and **9**. This is a strong indicator that the ΔD values are not necessarily correlated with $\Delta\delta$ values. The amine **10** presented a huge $\Delta\delta$ in comparison with **12**, on the other hand, the ΔD is smaller in **10** than in **12**. This effect can be attributed to the hydrogen bond capability of **10**, this interaction (N---HO) is very stable and the steric hindrance of BINOL is small, so both enantiomers of **10** bind with BINOL and the ΔD is small. The sulfoxide compound also showed baseline separation ($\Delta\delta$ = 8.9 Hz) but a ΔD of only 0.2 × 10^{-10} m^2s^{-1}. For compounds **12-22**, when using CSAs **1** and **2** a range of $\Delta\delta$ was observed from 0.0 Hz in compound **17** to 4.5 Hz in compound **16**, but once again, the $\Delta\delta$ values showed no correlation with the ΔD when comparing different samples. Mandelic acid (**22**) is a great example of how larger CSAs do not lead to better separation of signals in diffusion measurements. Using CSAs **1** and **2** the signals for analyte **22** were separated by 4.7 Hz in ^{1}H NMR spectra and 0.3 × 10^{-10} m^2s^{-1} in the diffusion map. For CSAs **3** and **4**, the separation in the 1D spectra was 2.6 Hz and 1.2 × 10^{-10} m^2s^{-1} in the diffusion maps. However, for CSA **5** the separation in the ^{1}H NMR spectrum was huge compared to CSAs **1-4** (96.4 Hz), but in the diffusion dimension, the signals were only 0.2 × 10^{-10} m^2s^{-1} apart.

Compounds **13-15** have a methoxyl substituent in positions 2', 3' and 4' in the phenyl ring and compounds **16-18** are nitro substituted in the same positions. From these six compounds, the first observation is that the substituents have no observable electronic effects in the ΔD values, but comparing the *ortho*-substituted compounds with *meta*- or *para*-substituted (Table S1, entries 8 versus 9 and 10, 11 versus 12 and 13, and even 15 versus 19 and 23), the *ortho*-substituted compounds have small ΔD values. This difference can be attributed to steric effects of the substituent that hinders the CSA approximation to nearby hydroxyl groups, inhibiting the hydrogen bond formation.

An alternative to sort out the overlap problem is to observe the ^{19}F nucleus instead of ^{1}H. Fluorine is very sensitive to changes in the chemical environment, its chemical shift ranges for at least 300 ppm for regular organic compounds. In addition, ^{19}F nucleus has a gyromagnetic ratio close to hydrogen and 100% of natural abundance, resulting in signal-to-noise ratio comparable with ^{1}H NMR. For compounds **19-21** the ^{19}F-{^{1}H}-DOSY was also acquired and comparing the entries pairs 32-33, 34-35, 36-37, 38-39, 40-41, 42-43 and 44-45 (Table S1 from supporting information), there is a great change in ΔD values when analyzing the ^{19}F nuclei in comparison to ^{1}H. This difference is somewhat unusual at first glance because the diffusion coefficients should be the same, once it was measured in the

same conditions and using the same sample. However, in the ^{19}F-{^{1}H} NMR spectra, the signals are more separated than in ^{1}H leading to a better fitting of the exponential decays and thus, diffusion coefficients measured more accurately.[18]

The importance of fluorine analysis is easily seen in compound **19**. The pulse sequence employed to acquire the DOSY experiments has no fluorine decoupling, so the methyl signal has a coupling constant with the benzylic hydrogen and another constant with the fluorine, which precludes the ^{1}H analysis, but ^{19}F-{^{1}H}-DOSY allows the diffusion analysis of compounds **19-21** (Fig. S45).

The separation of signals in ^{19}F-{^{1}H} spectra for the three compounds were observed only using CSA **5**, CSAs **1** and **2** differentiated only the enantiomers of compounds **20** and **21**. For the diffusion experiments, the ΔD when observing the ^{19}F nuclei was greater than the measurement observing the ^{1}H nuclei, since there is no signal overlap and signal decay is due to diffusional process.

Curiously, for compounds **20** and **21**, a better enantiomer differentiation in diffusion dimension was observed using a cheaper CSA, BINOL (**1** or **2**), as in comparison to an expensive CSA (**5**). This is unusual because as the molecular weight of the CSA grows, the observed diffusion coefficient of the diastereoisomeric complex should get smaller, but in this case, the ΔD is smaller when using **5**. So, the observed ΔD depends not only on the hydrogen bond strength of each diastereoisomeric complex and the molecular weight of the CSA, but it also depends on the enantioselectivity of the CSAs interactions with the analyte. In the worst-case scenario, without enantioselectivity, the CSA will interact equally with both enantiomers and no separation will be observed. On the other hand, in the best-case scenario, with an enantiospecific interaction, the CSA will interact with only one enantiomer and its diffusion coefficient will be significantly reduced.

The MAD methodology has proven to be very effective to discriminate enantiomers and investigate which enantiomer interacts more strongly with a given CSA. An inexpensive CSA was used, and even with severe overlaps, it was possible to measure diffusion coefficients for different diastereoisomeric complexes, which eliminates the requirement of baseline separation if the goal is to detect the enantiomeric pair in a mixture of compounds. From the experiments with aromatic compounds, it was concluded that the substituent has some influence on the ΔD value, possibly due to a competition of the hydroxyl groups and the substituents for the binding site of the CSA. For the diffusion experiments, even though it is possible to measure ΔD with overlapping signals, if the Δδ is greater than the signal broadening in singlets or the *J*-coupling in multiplets, the diffusion coefficients can be measured with increased accuracy. Finally, using different CSAs we were able to understand that the molecular weight of the CSA is not directly related to discrimination on diffusion dimension, but the strength of the non-covalent bond has to be taken into account.

The authors gratefully acknowledge the financial support from FAPESP (#2015/08541-6) and CAPES for the scholarship to KSS and CNPq for the fellowship to CFT.

Conflicts of interest

View Article Online
DOI: 10.1039/C9CC04268G

There are no conflicts to declare.

Notes and references

1 J. Szyszkowiak and P. Majewska, *Tetrahedron: Asymmetry*, 2014, **25**, 103.
2 J. M. Seco, E. Quiñoá, and R. Riguera, *Chemical Reviews*, 2012, **112**, 4603.
3 P. Lesot, C. Aroulanda, H. Zimmermannb, and Z. Luz. *Chemical Society Reviews*, 2015, **44**, 2330.
4 L. Fang, C. Lv, G. Wang, L. Feng, P. Stavropoulos, G. Gao, L. Ai, and J. Zhang, *Organic Chemistry Frontiers*, 2016, **3**, 1716.
5 L. Bai, P. Chen, J. Xiang, J. Suna, and X. Lei, *Organic & Biomolecular Chemistry*, 2019, **17**, 1466.
6 (*a*) N. Jain, A. N. Khanvilkar, S. Sahoo, and A. V. Bedekar, *Tetrahedron*, 2018, **74**, 68; (*b*) E. Tayama and T. Sugawara, *European Journal of Organic Chemistry*, 2019, 803; (*c*) S. Ito, M. Okunoa, and M. Asami, *Organic & Biomolecular Chemistry*, 2018, **26**, 213; (*d*) S. R. Chaudhari and S. N. Suryaprakash, *Journal of Molecular Structure*, 2013, **1033**, 75.
7 M. Seo, S. Jang, and H. Kim, *Chemical Communications*, 2018, **54**, 6804.
8 (*a*) Ref. 5; (*b*) Y. Zhu, X. Wu, S. Gu, and L. Pu, *Journal of the American Chemical Society*, 2019, **141**, 175; (*c*) T. Ema, D. Tanida, and T. Sakai, *Journal of the American Chemical Society*, 2007, **129**, 10591.
9 (*a*) Z. Chen, H. Fan, S. Yang, G. Bian, and L. Song, *Organic & Biomolecular Chemistry*, 2018, **16**, 8311; (*b*) L. Feng, G. Gao, H. Zhao, L. Zheng, Y. Wang, P. Stavropoulos, L. Ai, and J. Zhang, *The Journal of Organic Chemistry*, 2018, **83**, 13874; (*c*) G. Li, J. Cao, W. Zong, X. Lei, and R. Tan. *Organic Chemistry Frontiers*, 2016, **3**, 96.
10 (*a*) I. Pal, S. R. Chaudhari, and N. Suryaprakash, *New Journal of Chemistry*, 2014, **38**, 4908; (*b*) G. Bian, S. Yang, H. Huang, H. Zong, L. Song, H. Fan, and X. Sun, *Chemical Science*, 2016, **7**, 932.
11 S. R. Chaudhari, Srinivasa, and N. Suryaprakash, *RSC Advances*, 2012, **2**, 8689.
12 T. M. Barbosa, G. A. Morris, M. Nilsson, R. Rittner, and C. F. Tormena, *RSC Advances*, 2017, **7**, 34000.
13 L. Castañar, P. Moutzouri, T. M. Barbosa, C. F. Tormena, R. Rittner, A. Phillips, S. Coombes, M. Nilsson, and G. A. Morris, *Analytical Chemistry*, 2018, **90**, 5445-5450.
14 R. Evans and I. J. Day, *RSC Advances*, 2016, **6**, 47010.
15 G. Uccello-Barretta, F. Balzano, J. Martinelli, M. Berni, C. Villani, and F. Gasparrini, *Tetrahedron: Asymmetry*, 2005, **16**, 3746.
16 B. A. Jones, T. Balan, J. D. Jolliffe, C. D. Campbell, and M. D. Smith, *Angewandte Chemie International Edition*, 2019, **58**, 4596.
17 T. M. Barbosa, R. Rittner, C. F. Tormena, G. A. Morris and M. Nilsson, *RSC Advances*, 2016, **6**, 95173.
18 The use of fluorine-19 instead of proton to measure diffusion coefficients by NMR has already been discussed: (*a*) G. Dal Poggetto, V. Antunes, M. Nilsson, G. A. Morris, and C. F. Tormena, *Magnetic Resonance in Chemistry*, 2017, **55**, 323; (*b*) G. Dal Poggetto, D. C. Favaro, M. Nilsson, G. A. Morris, and C. F. Tormena, *Magnetic Resonance in Chemistry*, 2014, **52**, 172; (*c*) C. Dalvit and A. Vulpetti, *Magnetic Resonance in Chemistry*, 2012, **50**, 592.

View Article Online
DOI: 10.1039/C9CC04268G